17th World Conference on Earthquake Engineering, 17WCEE
Sendai, Japan - September 13th to 18th 2020
Paper N° C000073
Registration Code: S-A02341

# NUMERICAL MODELLING OF CAVITY WALL METAL TIES

O. Arslan[1,2], F. Messali[3], E. Smyrou[4], I. E. Bal[5], J. G. Rots[6]

[1] *Ph.D. Candidate, Faculty of Civil Engineering and Geosciences, Delft University of Technology, Delft, the Netherlands, o.arslan@tudelft.nl*
[2] *Researcher, Research Centre for Built Environment NoorderRuimte, Hanze University of Applied Sciences, Groningen, the Netherlands o.arslan@pl.hanze.nl*
[3] *Researcher/Lecturer, Faculty of Civil Engineering and Geosciences, Delft University of Technology, Delft, the Netherlands, F.Messali@tudelft.nl*
[4] *Associate Professor, Research Centre for Built Environment NoorderRuimte, Hanze University of Applied Sciences, Groningen, the Netherlands, e.smyrou@pl.hanze.nl*
[5] *Professor, Research Centre for Built Environment NoorderRuimte, Hanze University of Applied Sciences, Groningen, the Netherlands, i.e.bal@pl.hanze.nl*
[6] *Professor, Faculty of Civil Engineering and Geosciences, Delft University of Technology, Delft, the Netherlands, J.G.Rots@tudelft.nl*

...

## *Abstract*

The assessment of the out-of-plane response of unreinforced masonry (URM) buildings with cavity walls has been a popular topic in regions such as Central and Northern Europe, Australia, New Zealand, China and several other countries. Cavity walls are particularly vulnerable as the out-of-plane capacity of each individual leaf is significantly smaller than the one of a solid wall. In the Netherlands, cavity walls are characterized by an inner load-bearing leaf of calcium silicate bricks, and by an outer veneer of clay bricks that has only aesthetic and insulation functions. The two leaves are typically connected by means of metallic ties. This paper utilizes the results of an experimental campaign conducted by the authors to calibrate a hysteretic model that represents the axial cyclic response of cavity wall tie connections. The proposed numerical model uses zero-length elements implemented in OpenSees with the Pinching4 constitutive model to account for the compression-tension cyclic behaviour of the ties. The numerical model is able to capture important aspects of the tie response such as the strength degradation, the unloading stiffness degradation and the pinching behaviour. The numerical modelling approach in this paper can be easily adopted by practitioner engineers who aim to model the wall ties more accurately when assessing the structures against earthquakes.

*Keywords: Unreinforced masonry; Cavity walls; Numerical model; Wall ties*

## 1. Introduction

In recent years human induced earthquakes in the province of Groningen, located in the northern part of the Netherlands, have considerably increased, rendering critical the seismic response of unreinforced masonry (URM) structures. The majority of the existing buildings in that area is composed of URM and is not designed to withstand earthquakes. An extensive testing campaign was performed at TU Delft in 2015 to provide benchmarks for the Dutch situation [1]. The campaign aimed to investigate the behaviour of terraced houses built in the Netherlands during the period 1960-1980 [2,3,4] and characterized by the use of cavity walls. A cavity wall consists of two separate parallel walls, with an inner load-bearing masonry wall and an outer veneer mostly with aesthetic and insulating function (Fig. 1). The inner and outer walls are connected by metal ties, as prescribed in NEN-EN 845-1 [5].

The out-of-plane failure of URM walls is a common mechanism during an earthquake that often stems from poor wall-to-wall, wall-to-floor or wall-to-roof connections that provide insufficient restraint and boundary conditions. Cavity walls are particularly vulnerable to the out-of-plane mechanism because of the capacity of the wall ties as well as the slender geometry of the two parallel leaves.

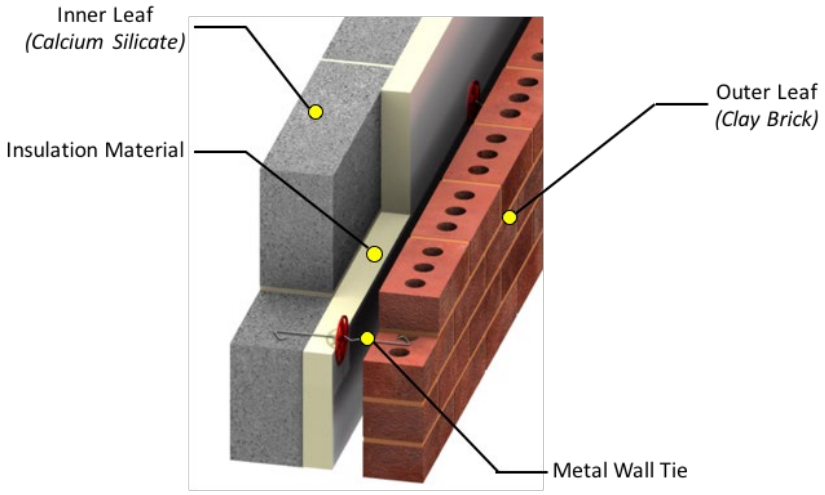


Fig. 1 – Cavity wall

Reneksis and Lafave [6] utilized the test data from Choi and Lafave [7] to develop and calibrate nonlinear finite element models that represented the full-scale experimental brick veneer wall panel specimens. They found that the tie could be modelled by axial links, with nonlinear material properties based on the observations of the test. It was concluded that brick veneer wall damage could be captured at various stages by examining whether the tie connections at key locations in the models exceeded their ultimate load and/or specific displacement capacities. Jo [8] developed a simplified finite element model in OpenSees that was calibrated using the test results conducted by the author to represent the in-plane and out-of-plane wall system behaviour of concrete masonry unit-tie-masonry veneer wall systems. The ties were modelled as truss elements with general hysteretic material behaviour. Okail et al. [9] developed a series of OpenSees models to simulate the seismic behaviour of brick veneers connected to a wood frame by means of metal ties. Beam-column elements with fibre cross section were used to model the masonry veneer, whereas the wood shear walls were simulated through elastic beam elements. The metal tie connections were modelled via nonlinear truss elements. A proper hysteretic model was selected to simulate the cyclic behaviour of the metal ties. The numerical model showed a good match with the experimental data. Based on the results, it was found that the connection force distribution was dependant on the cracking of the veneer.

The current study aims at a computationally efficient approach to simulate the experimental results of wall connections in cavity walls under cyclic loading representative of earthquake motions. The study is supported by the experimental work conducted by Arslan et al. [10] and by the mechanical model proposed by

Arslan et al. [11]. The open code OpenSees software [12] has been used in this study, but the proposed backbone curve can be easily adopted in most of the structural analysis software used in earthquake engineering. The backbone curve provides engineers and researchers with the mechanical model that can predict the force-displacement response for different typologies in terms of characteristic parameters, such as stiffness, strength and displacement.

## 2. Mechanical Model

A mechanical model for the cavity wall tie connections was proposed by the authors [11] in order to determine the load–displacement curve of the connection under axial load. The mechanical model describes the structural behaviour of the wall connections with calcium silicate bricks (CS) and solid clay bricks (CB) in terms of force-displacement behaviour and failure mechanism. The model has been calibrated and validated against the experiments conducted by the authors on the cavity wall tie at TU Delft [10].

Considering all the failure mechanisms and the experimental results, a simplified envelope curve was proposed for each typology to better fit the results obtained from the experimental campaign. The proposed curve was obtained by averaging the data from the experimental results. The force-displacement curve is idealized into trilinear branches in tension (elastic, hardening and post-peak phase) and by bilinear branches in compression (elastic and post-peak phase). For defining the curve shown in Fig. 2, ten material parameters are required. These are:

(i) elastic force in tension, $F_{Te}$
(ii) peak force in tension, $F_T$
(iii) ultimate failure force in tension, $F_{Tu}$
(iv) displacement at elastic force in tension, $\Delta_{Te}$
(v) displacement at peak force in tension, $\Delta_T$
(vi) displacement at ultimate failure force in tension, $\Delta_{Tu}$
(vii) peak force in compression, $F_C$
(viii) residual force in compression, $F_{Cu}$
(ix) displacement at peak force in compression, $\Delta_C$
(x) displacement at residual force in compression, $\Delta_{Cu}$

The proposed curve is valid for CS and CB for all failure modes. However, the calibration of these parameters for the envelope curve are different for CS and CB walls.

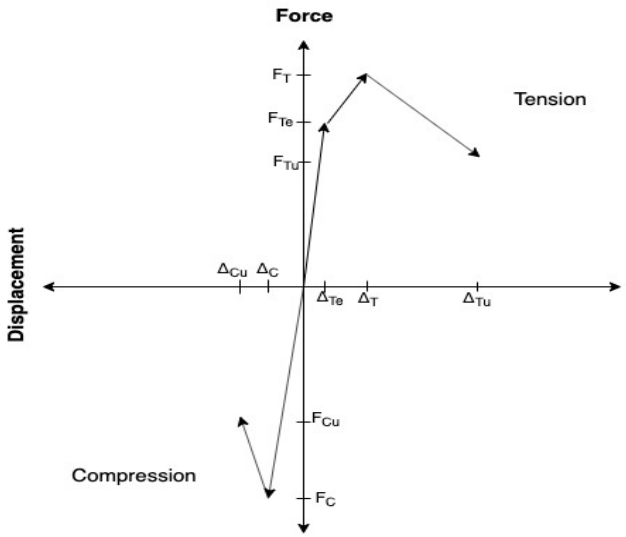


Fig. 2 – Simplified envelope curve

The equations for computing the parameters of the simplified envelope curve are provided in a tabular form (Table 1). The proposed mechanical model can adequately predict the force-displacement behaviour obtained from the tests.

Table 1 – Equations for the parameters of the proposed curve for each typology

| Number of equation | Parameter | Equation | Validated typology |
|---|---|---|---|
| 1 | $F_{Te}$ | $a \times \sqrt{f_c} \times \pi \times \phi \times L_S$ | CS70, CS50, CB50, CS70-15D |
| 2 | $F_T$ | $F_{Te} + \frac{4}{L_H} \times (\frac{f_c \times \phi \times {L_H}^2}{2} + \frac{\sigma_y \times \pi \times \phi^3}{32})$ | CS70, CS50 |
| 3 | $F_T$ | $F_{Te} + \frac{4}{L_H} \times (\frac{f_c \times \phi \times {L_H}^2}{2} + \frac{\sigma_y \times \pi \times \phi^3}{32}) + \frac{24 \times E \times I \times \phi}{{L_C}^2}$ | CS70-15D |
| 4 | $F_T$ | $F_{Te} + f_c \times \phi \times L_S$ | CB50 |
| 5 | $F_{Tu}$ | $F_T \times 0.8$ | CS70, CS50, CB50, CS70-15D |
| 6 | $\Delta_{Te}$ | 1 | CS70, CS50, CB50, CS70-15D |
| 7 | $\Delta_T$ | $1 + \frac{L_H}{4}$ | CS70, CS50, CS70-15D |
| 8 | $\Delta_T$ | $1 + \frac{L_s}{10}$ | CB50 |
| 9 | $\Delta_{Tu}$ | $0.8 * \Delta_T + 10$ | CS70, CS50, CB50, CS70-15D |
| 10 | $F_C$ | $\frac{\pi^2 \times E \times I}{K^2 \times {L_C}^2}$ | CS70, CS50, CB50 |
| 11 | $F_C$ | $\frac{\pi^2 \times E \times I}{K^2 \times {L_C}^2} - \frac{24 \times E \times I \times \phi}{{L_C}^2}$ | CS70-15D |
| 12 | $F_{Cu}$ | $F_C \times 0.8$ | CS70, CS50, CB50, CS70-15D |
| 13 | $\Delta_C$ | 1 | CS70, CS50, CB50, CS70-15D |
| 14 | $\Delta_{Cu}$ | $0.8 * \Delta_C + 2$ | CS70, CS50, CB50, CS70-15D |

Note: CS70 = the hooked part of the tie is embedded in CS, with 70mm anchoring length. CS70-15D = the hooked part is embedded in CS, with 70mm, the zig-zag end of the tie is bent 15°. CS50 = the hooked part is embedded in CS, with 50mm. CB-50 = the zig-zag part of the tie is embedded in CB, with 50mm

## 3. Numerical Analyses

The experimental results of tie response in CS and CB units have been simulated in this work within the OpenSees environment [12]. In order to do that, the average experimental curves were fit into zero-length element backbone curves as explained below.

The force-displacement curves defined for monotonic loading differ from the envelope curves for cyclic loading by the cumulative damage in cycling loading. The backbone curves for each tested typology shown in Fig. 3, force-displacement curves of the quasi-static tests are given together with the experimental backbone curves presented previously by the authors [10] and the simplified curve proposed by the authors [11]. The backbone curves for cyclic and monotonic were presented separately for CS and Clay specimens by the author [10]. However, the proposed curve is valid for each typology.

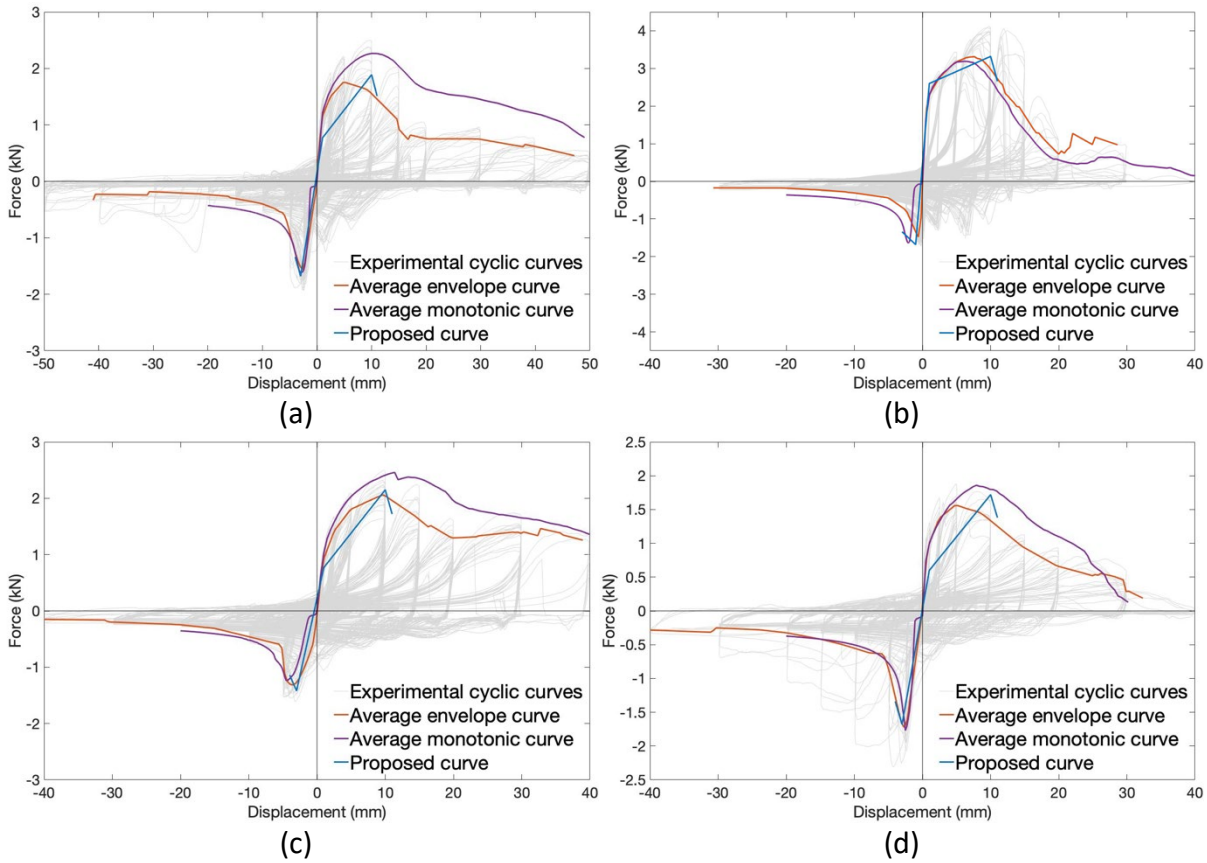


Fig. 3 – Average force-displacement envelope curve for monotonic and cyclic loading with the prosed curve for CS70 (a), CB50 (b), CS70-15D (c) and CS50 (d)

The "Pinching4" model [13] was chosen as material model due to the pinching effect and the degradation in strength and stiffness under cyclic loading. The properties of the Pinching4 material in Opensees are shown in Fig. 4 [12,13] and define a backbone curve, the unloading-reloading path that represents the pinching behaviour, and the parameters for strength and stiffness degradation. The curve proposed in this paper is hence created by inserting appropriate variables into the Pinching4 material in OpenSees.

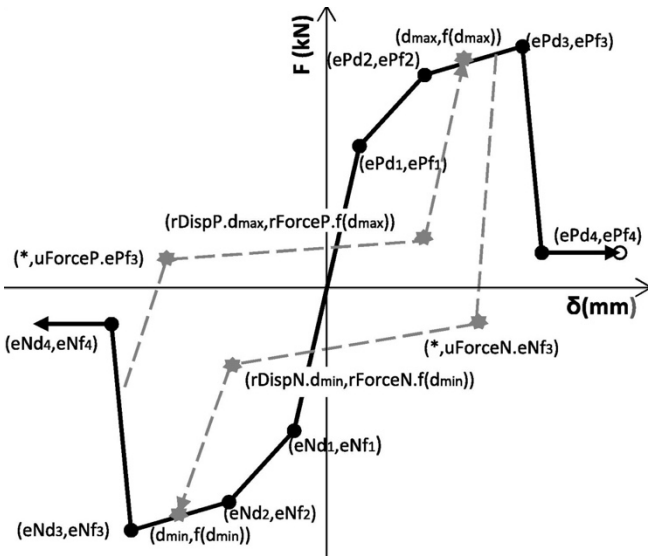


Figure 4. Pinching Material model in OpenSees [12]

The Pinching4 constitutive law described above was used in zero-length element to simulate the wall connection behaviour. The zero-length elements considered for this simulation correspond to springs with only one degree of freedom (DOF), i.e. the axial response, having a hysteretic response that is defined by using the calibrated Pinching4 material. The other DOFs in the model are left constrained.

The tension backbone curves differ from the compression backbone curves for each tested typology due to the different failure mechanisms in tension and compression. Therefore, the backbone curve should be defined separately in tension and compression for each typology in Pinching4 material. However, the strength and stiffness degradation parameters cannot be defined separately in tension and compression due to limitation of the Pinching4 constitutive law. The material parameters were hence calibrated in order to match the overall simulated responses from the experimental results.

Due to its flexible format, the Pinching4 material can actually successfully fit to a wide variety of experiment results. The point of this study is to propose a general model by using an averaging procedure. In order to do this, the backbone shape given in Fig. 2 has been fitted to every tested typology individually and the input parameters have been found for the best fit. As an example, an experimental hysteresis was chosen from one of those typologies to validate the numerical model with the experimental data (Fig. 5).

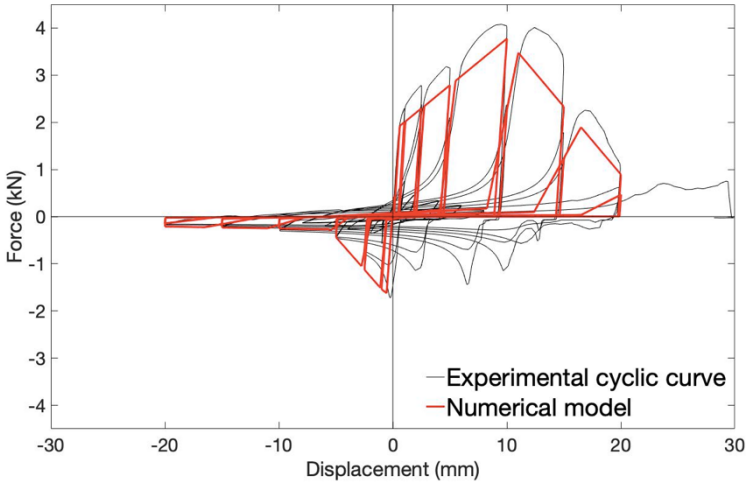


Figure 5. Comparison between experimental and numerical result

Additional parameters of the Pinching4 model define the cyclic response. Two parameters, rDisp and fForce, define the ratio of the deformation/force at which the reloading starts to the maximum deformation/force demand of the previous cycle in the loading direction of interest for positive and negative. The uForce parameter defines the ratio of strength developed after unloading from the negative/positive load to the maximum strength developed under monotonic loading. The cyclic deterioration for unloading, reloading stiffness and strength are controlled with gKLim, gDLim, and gFLim, respectively. The values of cyclic degradation parameters (gKLim, gDLim, and gFLim) and pinching parameters (rDispP, rDispN, rForceP, rForceN, uForceP and uForceN) simulate the force-deformation history for selected specimens. The values suggested for all these parameters are reported in Table 2.

Table 2 – Suggested values of the modelling parameters for OpenSees Pinching4 material based on experiments and mechanical model (number of the equation from the mechanical model between brackets)

| **Parameters** | **Suggested Values** | **Suggested Values** | **Suggested Values** | **Suggested Values** |
|---|---|---|---|---|
| | CS70 | CB50 | CS70-15D | CS50 |
| **Positive backbone** | | | | |
| $ePf_1$ (kN) | 0.77 [1] | 2.16 [1] | 0.77 [1] | 0.60 [1] |
| $ePf_2$ (kN) | 1.89 [2] | 3.32 [4] | 2.15 [3] | 1.72 [2] |
| $ePf_3$ (kN) | 1.51 [5] | 2.66 [5] | 1.72 [5] | 1.38 [5] |
| $ePf_4$ (kN) | 0.80 | 0.50 | 1.50 | 0.90 |
| $ePd_1$ (m) | 0.001 [6] | 0.001 [6] | 0.001 [6] | 0.001 [6] |
| $ePd_2$ (m) | 0.01 [7] | 0.01 [8] | 0.01 [7] | 0.01 [7] |
| $ePd_3$ (m) | 0.011 [9] | 0.011 [9] | 0.011 [9] | 0.011 [9] |
| $ePd_4$ (m) | 0.011 | 0.025 | 0.04 | 0.011 |
| **Negative backbone** | | | | |
| $eNf_1$ (kN) | -1.68 [10] | -1.68 [10] | -1.42 [11] | -1.68 [10] |
| $eNf_2$ (kN) | -1.34 [12] | -1.34 [12] | -1.10 [12] | -1.34 [12] |
| $eNf_3$ (kN) | -0.60 | -0.30 | -0.60 | -0.60 |
| $eNf_4$ (kN) | -0.10 | -0.10 | -0.10 | -0.10 |
| $eNd_1$ (m) | -0.003 [13] | -0.001 [13] | -0.003 [13] | -0.003 [13] |
| $eNd_2$ (m) | -0.004 [14] | -0.003 [14] | -0.004 [14] | -0.004 [14] |
| $eNd_3$ (m) | -0.005 | -0.0056 | -0.005 | -0.005 |
| $eNd_4$ (m) | -0.04 | -0.050 | -0.040 | -0.040 |
| **Pinching** | | | | |
| rDispP | 0.95 | 0.53 | 0.53 | 0.53 |
| fForceP | 0.22 | 0.20 | 0.20 | 0.20 |
| uForceP | 0.04 | 0.05 | 0.09 | 0.09 |
| rDispN | 0.80 | 0.70 | 0.76 | 0.76 |
| fForceN | 0.53 | 0.66 | 0.66 | 0.66 |
| uForceN | 0.04 | 0.70 | 0.94 | 0.90 |
| **Unloading stiffness degradation** | | | | |
| $gK_1$ | 0.15 | 0 | 0 | 0 |
| $gK_2$ | 0.15 | 0.1 | 0.1 | 0.1 |
| $gK_3$ | 0.15 | | 0 | 0 |
| $gK_4$ | 0.15 | 0.1 | 0.1 | 0.1 |
| gKLim | 0 | 0.2 | 0.1 | 0.1 |
| **Reloading stiffness degradation** | | | | |
| $gD_1$ | 0.1 | 0.2 | 0.1 | 0.1 |
| $gD_2$ | 0.2 | 0.2 | 0.1 | 0.1 |
| $gD_3$ | 0.1 | 0.2 | 0.1 | 0.1 |
| $gD_4$ | 0.2 | 0.2 | 0.1 | 0.1 |
| gDLim | 0.1 | 0.1 | 0.1 | 0.1 |
| **Strength degradation** | | | | |
| $gF_1$ | 0 | 0 | 0 | 0 |
| $gF_2$ | 0 | 0 | 0 | 0 |
| $gF_3$ | 0 | 0 | 0 | 0 |
| $gF_4$ | 0 | 0 | 0 | 0 |
| gFLim | 0 | 0 | 0 | 0 |
| Energy degradation (gE) | 10 | 10 | 10 | 10 |
| **Damage type** | Cycle | Cycle | Cycle | Cycle |

The average cyclic hysteresis curves, obtained following the procedure and using parameters described above, are presented in Fig. 6 for each tested typology of wall connections. The figure shows that the results obtained with numerical analyses have a fairly good match with the average experimental curves. The calibrated hysteretic models are capable of capturing important aspects of the tie response, such as the initial stiffness, strength, sudden drop of strength and cyclic response in the degradation part of the response. However, the Pinching4 material is not capable of accurately capturing the unloading-reloading paths of the cyclic responses from tension to compression which is governed by the buckling deformation.

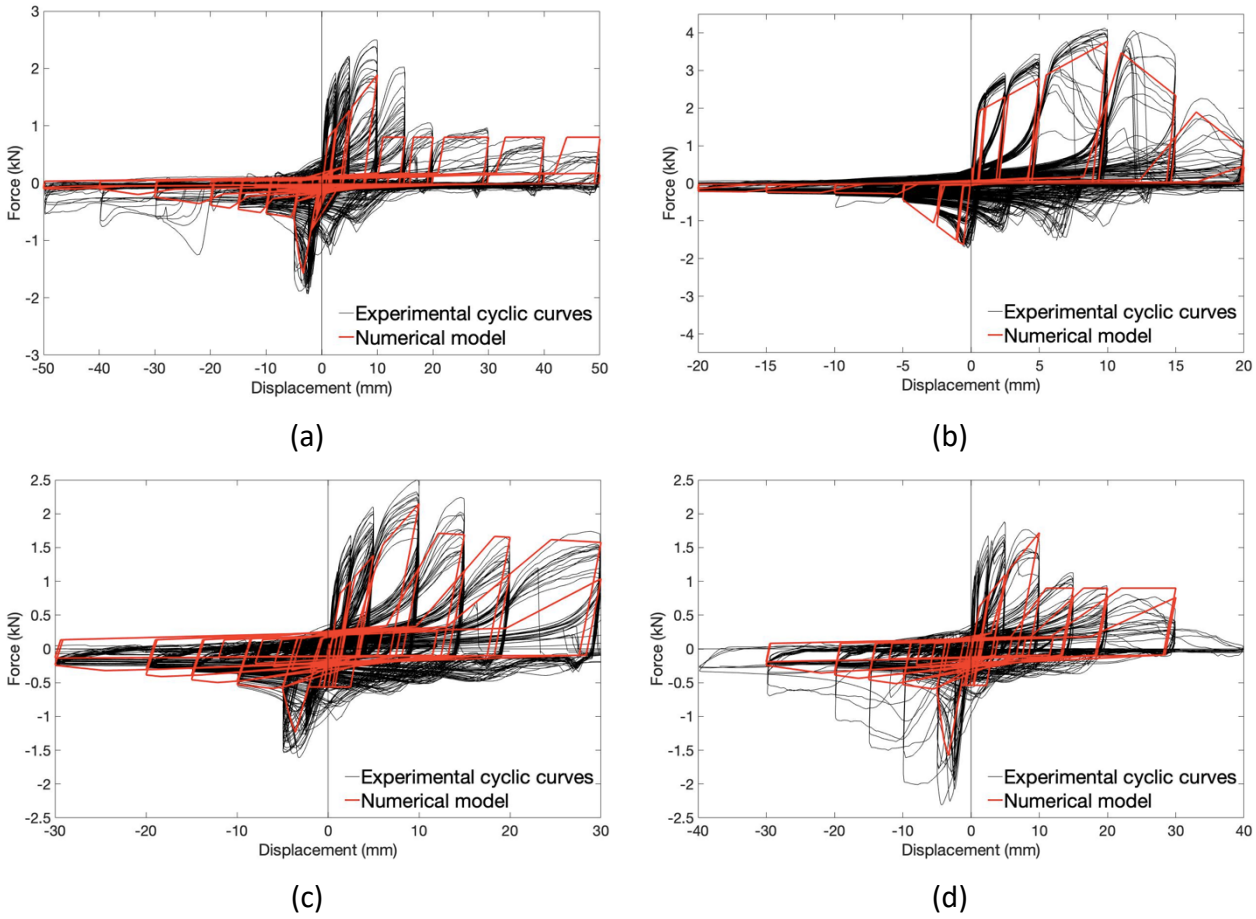


Figure 6. Simulated and experimental response for CS70 (a), CB50 (b), CS70-15D (c) and CS50 (d)

A comparison of the accumulated hysteretic energy (i.e. the area within the hysteresis loop) is given in Fig. 7, where it can be seen that the proposed numerical model performs well in terms of hysteretic energy dissipated by the wall connection. The numerical model dissipates more energy per cycle for smaller displacements whereas smaller energy dissipation is observed for larger displacements compared to the experimental results. This can be attributed to the lack of ability of the model to simulate accurately the unloading-reloading path from tension to compression after the buckling of the tie, as mentioned above, that determines the compressive peaks for positive displacements which are not captured by the Pinching4 constitutive model. At the end of the tests, the total energy dissipation for the numerical model is very close to the average peak energy dissipation for each tested typology.

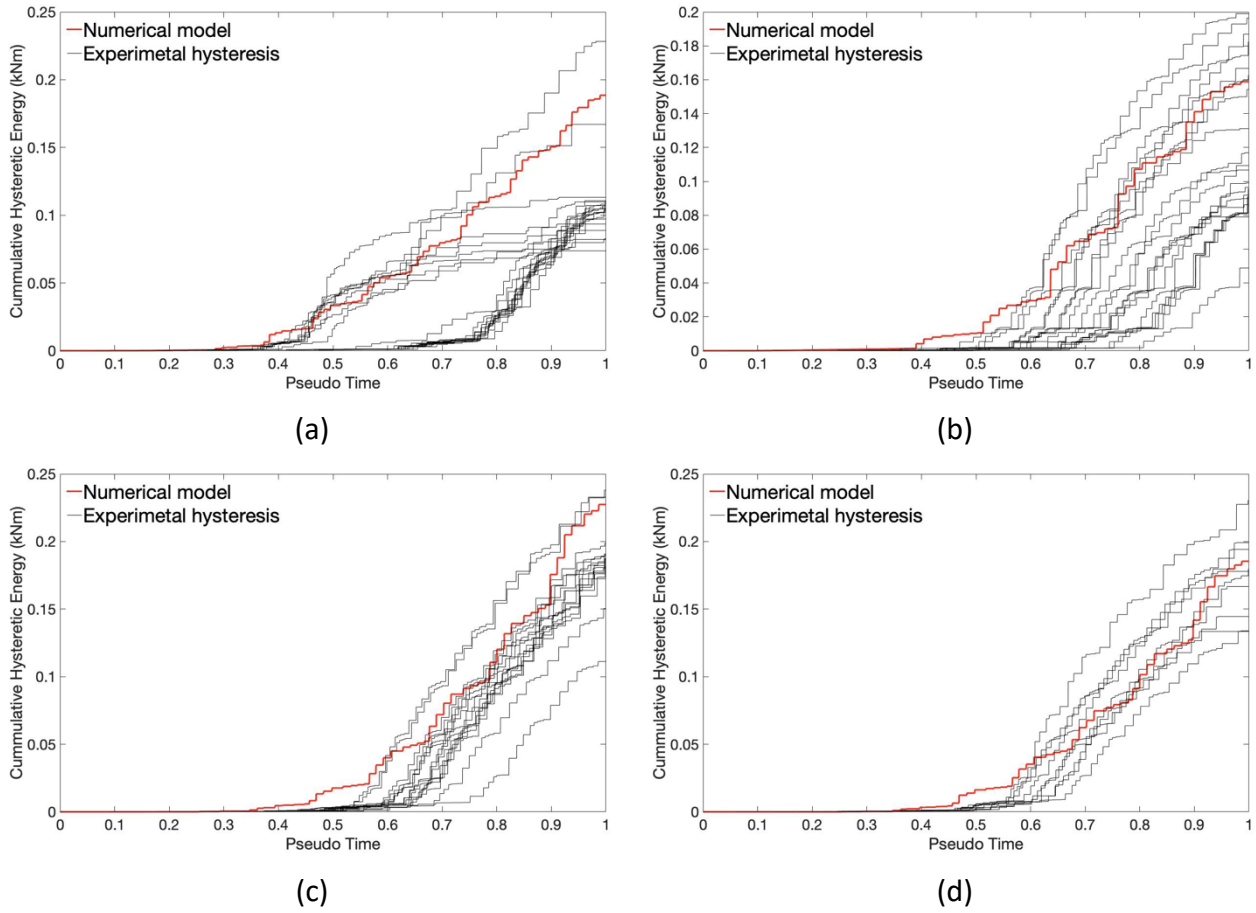


Figure 7. Cumulative hysteretic energy for experimental and numerical cyclic results for CS70 (a) and CB50 (b), CS70-15D (c) and CS50 (d)

## 4. Conclusions

Double-leaf cavity walls constitute a large portion of the building inventory in the Groningen gas field, an area in the north of the Netherlands subjected to induced earthquakes. The out-of-plane response of the double-leaf cavity walls is one of the most critical failure mechanisms for such buildings. The cavity walls are composed of a loadbearing inner leaf made of calcium silicate brick masonry and an outer leaf made of solid clay brick masonry. Wall-to-wall metallic ties can provide an efficient retain to the out-of-plane collapse of the single leaves, but their strength has not been widely investigated yet.

In this study, the mechanical model derived according to the experimental results of a previous testing campaign carried out by the authors are used to develop a general load-deformation hysteretic numerical model for different typologies of cavity wall connections. The numerical simulations make use of nonlinear zero-length spring elements, whose axial response is defined by a constitutive law (Pinching4) already implemented in the open code OpenSees. Alternatively, similar procedures can be adopted in other structural analysis software used in earthquake engineering. The material parameters of the Pinching4 law are derived from the experimental tests. The strength degradation, stiffness degradation and pinching behaviour of the load-deformation response are modelled differently for each typology and are able to reproduce adequately the observed experimental force displacement curves. However, the description of the unloading-reloading path from tension to compression may be modified to better capture the buckling response of the ties.

The authors believe that the hysteretic model can be used by structural engineers for an accurate modelling of the response of wall-to-wall connections under dynamic earthquake loading.

## 5. References

[1] Messali F, Esposito R, Jafari S, Ravenshorst GJP, Korswagen P, Rots JG (2018): A multiscale experimental characterisation of Dutch unreinforced masonry buildings. *Proc., 16th European Conference on Earthquake Engineering (ECEE)*, Thessaloniki, Greece.

[2] Rots JG, Messali F, Esposito R, Mariani V, Jafari S (2017): Multi-Scale Approach towards Groningen Masonry and Induced Seismicity. *Key Engineering Materials*, **747**, 653-661.

[3] Esposito R, Terwel KC, Ravenshorst GJP, Schipper HR, Messali F, Rots JG (2017): Cyclic pushover test on an unreinforced masonry structure resembling a typical Dutch terraced house. *Proc., 16th World Conference on Earthquake*, Santiago, Chile.

[4] Messali F, Ravenshorst GJP, Esposito R, Rots JG (2017): Large-scale testing program for the seismic characterization of Dutch masonry walls. *Proc., 16th World Conference on Earthquake (WCEE)*, Santiago, Chile.

[5] NEN-EN 845-1 (2016), Specification for ancillary components for masonry - Part 1: Wall ties, tension straps, hangers and brackets, Nederlands Normalisatie-instituit (NEN).

[6] Reneckis D, LaFave JM (2005): Analysis of brick veneer walls on wood frame construction subjected to out-of-plane loads. *Construction and Building Materials*, **19**, 430-447.

[7] Choi YH, LaFave JM (2004): Performance of corrugated metal ties for brick veneer wall systems. Journal of Materials in Civil Engineering, **16** (3): 202.

[8] Jo S (2010): Seismic behavior and design of low-rise reinforced concrete masonry with clay masonry veneer. *Ph.D Dissertation*.University of Texas, Austin.

[9] Okail H (2010): Experimental and analytical investigation of the seismic performance of low-rise masonry veneer buildings. *Ph.D Dissertation*, University of California, San Diego, USA.

[10] Arslan O, Messali F, Smyrou E, Bal IE, Rots JG (2020): *Experimental Characterization of Masonry Wall Metal Tie Connections in Double-Leaf Cavity Walls*. Manuscript submitted for publication.

[11] Arslan O, Messali F, Smyrou E, Bal IE, Rots JG (2020): Mechanical modelling of cavity wall metal ties. *Submitted to the 17th International Brick and Block Masonry Conference, 17IB2MaC,* Krakow, Poland.

[12] Mazzoni S, McKenna F, Scott MH, Fenves GL (2009): Open System for Earthquake Engineering Simulation User Command-Language Manual, OpenSees Version 2.0, Berkeley, California.

[13] Lowes L, Mitra N, Altoontash A (2004): A Beam-Column Joint Model for Simulating the Earthquake Response of Reinforced Concrete Frames, *PEER Report 2003/10*, Pacific Earthquake Engineering Research Center, Berkeley, USA.